

# Bruise Detection in Apples Using Infrared Imaging

Sourav Dey Roy,<sup>1</sup> Dipak Hrishi Das,<sup>2</sup> Mrinal Kanti Bhowmik<sup>1,\*</sup> and Anjan Kumar Ghosh<sup>3</sup>

<sup>1</sup>Department of Computer Science and Engineering, Tripura University (A Central University), Suryamaninagar-799022, Tripura (W), India

<sup>2</sup>Department of Information Technology, Bir Bikram Memorial College, Agartala-799004, Tripura(W), India

<sup>3</sup>Tripura University (A Central University), Suryamaninagar-799022, Tripura (W), India

souravdeyroy49@gmail.com, dhdcse@gmail.com, \*mrinalkantibhowmik@tripurauniv.in and anjn@ieee.org

**Abstract**— Defects in apples cause food safety concerns touching the general public and strongly affect the commodity market. Due to the increasing incidence, the detection of bruises is a challenge now a day's especially when the bruises are not visible externally. Infrared imaging provides an important window for detection of bruises that are not visible externally. The study has been investigated on the infrared images of both fresh and bruised apples. For our investigation, a new dataset has been designed by maintaining standard acquisition protocol to improve the potentiality and accuracy of the thermograms. The contribution of the investigation includes asymmetric analysis of the acquired thermograms using first and second order statistical analysis and fractal analysis of pre-processed thermograms. Automatic detection of the bruised region was done using anisotropic diffusion and K-means clustering for investigation of the spread of the bruised region.

**Index Terms**—Food quality; Apple; Bruise; Infrared Imaging; Statistical Analysis; Fractal Analysis; Segmentation

## I. INTRODUCTION

Information regarding the quality of the food is most important before consumption. Assessing the quality parameters is a big challenge since differentiating impurities or freshness of food is difficult. Apple is one of the largely cultivated tree fruits today and is recognized as an important economic fruit worldwide. The Food and Drug Administration (FDA) has approved apples which are resistant to bruises could have unknown risks to human health [1]. Bruising is defined as damage of fruit tissue as a result of external forces which cause physical changes of texture and/or chemical changes of colour, smell and taste. The factors depending on which mechanical damages of apples occurs are soil cultivation, nutrition and weather conditions in the field during fruit growth. Owing to the physical properties of apples, the bruises are not visible externally [2]. The parameters which cannot be well detected by visual inspection and physical separation because of affected by psychological factors such as fatigue or acquired habits, there is a high risk of human error in classification processes. This is one of the most important drawbacks that can be prevented by automated inspection systems based on computer vision. It is a challenging task to detect bruises on the fruit which usually take place under the fruit skin. Infrared Thermography (IT) offers a potential non-invasive, non-contact and radiation free imaging modality for assessment of abnormal infrared radiation from objects. Up to 100% of apple bruises were detected using thermal imaging by discriminating surface temperature between bruised and non-bruised tissues [3]. There are generally two approaches for non-destructive bruise detection using infrared imaging: passive and active [4]. Passive thermography consists of measurement of infrared radiation from the objects under natural conditions between

studied objects and surrounding air. On the other hand, active thermography consist of measurement of the infrared radiation after the object under study is heated by means of external source.

The paper mainly explores a non-invasive infrared imaging based automatic bruise detection using passive thermography. In our study, we have created our own dataset of bruise and fresh apples by following the standard thermogram capturing procedure. The acquisition setup is established at the Biomedical Infrared Image Processing Laboratory of Computer Science and Engineering Department of Tripura University (A Central University). The paper emphasizes on developing a statistical feature based analysis that can signify the presence of thermal asymmetry in the fresh and bruised apples. The developed method involves the extraction of eleven statistical features including both the first order and second order features. The structural asymmetry between both the types of apples (i.e. fresh and bruised apples) are analyzed using box counting method of fractal dimension. Automatic segmentation of the bruised region is carried out using anisotropic diffusion followed by k-means clustering and the spreadness of this area is measured in terms of area and fractal dimension.

The whole paper is organized as; Section II describes the literature survey on the computer aided techniques for detection of bruises in fruits. Section III elaborately describes the capturing procedure of the dataset used in the analysis. In Section IV methodology for asymmetric analysis and automatic bruised detection in the thermograms of apples has been illustrated. Section V reports the experimental results with discussion of the methodology. And finally, section VI concludes the paper.

## II. RELATED WORK

Detection of mechanical defects in apples plays a crucial role for quality inspection systems. In the recent years, the research communities have sparked off thunder for developing computer aided techniques to advance this area in terms of quality inspection and safety detection, and sorting of food. Some of these existing works are shown in TABLE I. Undergoing a number of research works, it has been found that detection of bruises is critical both to researchers and industry personnel in their work for development of the procedures to reduce this serious cause of loss. From the survey work it has been noticed that most of the researchers have concentrated on using hyperspectral imaging and very few work has been investigated on the infrared imaging based detection of bruises on apples. So in our work, we have created infrared imaging dataset of both bruised and non-bruised apples and performed statistical analysis for detecting the presence of asymmetry between both the types of apples.

TABLE I  
SURVEY TABLE OF DIFFERENT COMPUTER AIDED TECHNIQUES FOR QUALITY INSPECTION OF APPLES

| Author/ Year                    | Method Used  | Type of Image                             | Observation  | Accuracy/ Result   |
|---------------------------------|--|---|--|--|
| J. Xing et.al./ 2005 [5]        | Principal Components Analysis (PCA), Classification algorithm based on moments thresholding  | Multi-spectral Imaging System             | Found that among selected four bands of principal components (PCs), second and third PCs are suitable for detecting the presence of bruises in apples  | 86% accuracy   |
| B.L. Upchurch et.al./ 1994 [6]  | Feature extraction based on contrast of the images   | Near-Infrared (NIR) Imaging               | By comparing the contrast between two concentric circular profiles of bruised and unbruised areas, the changes in the NM reflectance were characterized.   | Not Provided   |
| J. Varith et.al. / 2013 [3]     | Thermal Diffusivity  | Thermal Imaging                           | The distinct temperature differences between bruised and sound tissues was due to the changes in thermal diffusivity.  | Not Provided   |
| B.S. Bennedsen et.al./ 2005 [7] | Thresholding Based Segmentation, Artificial Neural Network (ANN), Principal Components (PCs)   | Near-Infrared (NIR) Imaging               | The ability of the methods to find individual defects and measure the area ranged from 77 to 91% for the number of defects detected, and from 78 to 92.7% of the total defective area.   | Bruise Detection Rate of 77 and 91.6% , with 1.1–3.6% false positives. |
| J. Xing et.al./ 2007 [8]        | PCA, Contour Fill Algorithm, Morphological Operation   | Hyperspectral Imaging                     | The stem-end regions were identified from the cheek surfaces from the contour features of the first PC score images and none of the sound tissue was misclassified   | 98.33% classification accuracy   |
| G. ElMasry et.al./ 2008 [9]     | Partial Least Squares method , Discrimination analysis   | Hyperspectral Imaging                     | Based on the spectral data analysis, three wavelengths (750, 820, and 960nm) were chosen and observed that the selected group of wavelengths has a great discrimination power for bruise detection in different background colors. | 93.95% of the variance between normal and bruised spectral data.       |
| P. Baranowski et.al./ 2009 [4]  | Pulsed-Phase Thermography (PPT), Thresholding based Segmentation   | Thermal Imaging                           | The investigations have shown that active thermography is useful for detection of early bruises in apples.   | Not Provided   |
| P. Baranowski et.al./ 2012 [10] | PCA, Minimum Noise Fraction (MNF), Linear Discriminant Analysis (LDA), Support Vector Machine (SVM), Soft Independent Modelling of Class Analogy (SIMCA) | Hyperspectral Imaging and Thermal Imaging | They observed that Thermal MWIR imaging indicate the best prediction efficiency for bruise recognition.  | LDA: 95% accuracy<br>SVM: 92% accuracy<br>SIMCA: 67% accuracy          |

Also, structural analysis of the bruised apples are carried out by segmenting the bruised areas and measuring the spreadness in terms of area and dimension.

### III. DATA COLLECTION

#### A. Environmental Condition and Camera Setup for Thermogram Acquisition

There are several factors need to be considered while the acquisition of thermograms that can influence the analysis and evaluation of infrared images. Practically it is difficult to control all the factors are very much difficult, but being aware of those factors is essential in many context. The factors that affects the acquisition of the thermograms are:

- Specification of Infrared Camera
- Environmental Condition
- Position of Infrared Imaging System and Objects

In our study, the protocol which has been followed to create

a controlled environment in order to decrease the negative influence of the above mentioned three factors is shown in Fig.1. The camera has been mountain on a tripod stand with an alignment of 90° in between the camera and the area of imaging as shown in Fig. 2. To eliminate external infrared energy emitted from sources such as electric wires, pipes, outlets, etc., we made a background by black cloth which has been positioned behind the object. The size of the background has been fixed based on the Field of View (FOV) of the infrared camera and distance between the object and the camera.

#### B. Thermogram Dataset Description

Maintaining the above mentioned standard procedure, we have acquired the thermograms of apples in two different parts. In the first part, 50 fresh apples are bought from the market and thermograms of those apples are captured by stabilizing them at room temperature. After this, the apples are

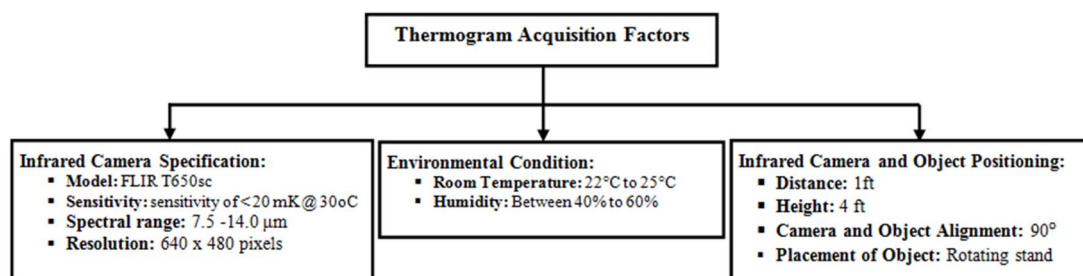


Fig. 1 Factors Affecting Thermogram Acquisition Standard

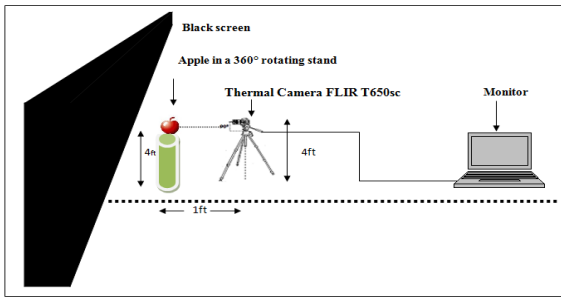


Fig. 2 Camera Setup and Positioning of the Object during Thermogram Acquisition

allowed to be bruised by keeping them at normal temperature for seven days and again the thermograms of those apples are captured by maintaining the same procedure. The thermograms of similar apples are captured on the twenty-first day. In the second part, 20 bruised apples that are almost rotten inside but are not visible externally are bought from the market as per instruction of the vendors and thermograms of those apples are captured by placing them in the rotating stand so that their bruised areas are detected. Some of the captured sample images are shown in Fig. 3. Here the first part of the database was used for asymmetric analysis of the thermograms and the second part of the database was used for automatic segmentation of the bruised area and to measure the spreadness of this area.

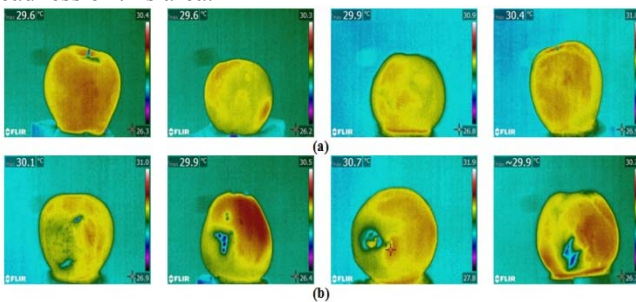


Fig. 3 Sample Images of Captured Thermograms (a) Fresh Apples; (b) Bruised Apples

#### IV. METHODOLOGY

##### A. Pre-processing of the thermograms

In the pre-processing stage, the thermograms of apples are cropped manually to a standard resolution of  $200 \times 200$  pixels so as to remove all the unnecessary parts except the object of interest. Then these cropped images are converted into gray scale image for further analysis so as to extract statistical and structural features and to segment the bruised areas from the thermograms as described in section B and C.

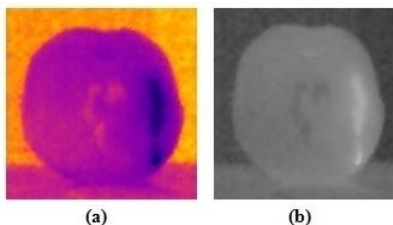


Fig. 4 Pre-Processing of the Thermograms (a) Original Image; (b) Pre-Processed Image

##### B. Asymmetric Analysis of the Thermograms

In this paper, the extraction of statistical features using first and second order statistical analysis and fractal dimension for

asymmetry analysis between bruised and fresh apples is conducted based on the evaluation of intensity distribution.

1) *First Order Statistical Feature Extraction*: The first order statistical features are also known as the Gray Level Histogram Based Statistical Features as they are directly computed from probability of occurrence of the gray levels in the images [12]. For first order statistical analysis we have calculated mean, variance, standard deviation, skewness, kurtosis and entropy of the thermograms.

2) *Second Order Statistical Feature Extraction*: The second order statistical features are extracted from the Gray Level Co-occurrence Matrix (GLCM) that deals with the relative positions of the gray levels within an image [11]. On the other hand inter-pixel distance, orientation and the spatial resolution of an image also plays a crucial role in the computation of co-occurrence matrices. For second order statistical analysis we have calculated contrast, homogeneity, energy, entropy and correlation of the thermograms.

3) *Fractal Feature Extraction using Box Counting method*: Fractal features can be effective in analyzing the difference in textures. For asymmetric analysis between bruised and fresh apples, fractal dimension is calculated using the most widely used box-counting technique that quantifies the space filling capacity of a fractal pattern. In box counting method, fractal dimension is the slope of the line when we plot the value of  $\log(N)$  on the Y-axis against the value of  $\log(r)$  on the X-axis. Here  $N$  is the number of boxes that cover the pattern, and  $r$  is the magnification or the inverse of the box size. The equation to denote the fractal dimension is given by [12]:

$$D = \frac{\log(N)}{\log(r)} \quad (1)$$

##### C. Automatic Segmentation of the Bruised Region

Segmentation of the bruised region plays a significant role in the analysis of the infrared images. However, automated detection of bruised region from images is a very challenging task due to the lack of clear limits in these images. From this viewpoint, we have taken two ideas, i.e., anisotropic diffusion and K-means clustering for extraction of the bruised region from the whole thermograms. The methodology for automatic segmentation of the bruised region of the acquired thermograms of apples has been illustrated in Fig. 5. The brief details of all the steps are described below.

1) *Smoothing using Anisotropic Diffusion*: For accurate extraction of the Region of Interest (ROI), the pre processed images are smoothed using anisotropic diffusion filtering to avoid the blurring and localization problem in the acquired thermograms. The discretized equation of Perona and Mallik anisotropic diffusion is as follows [13]

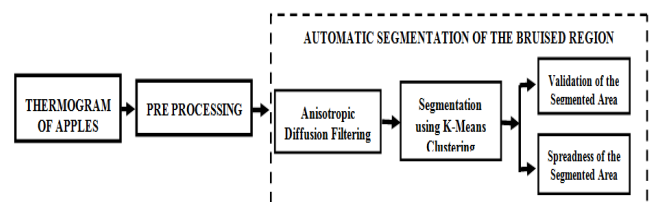


Fig. 5 Block Diagram of the Proposed Methodology for Automatic Segmentation of the Bruised Region

TABLE II  
ASYMMETRIC ANALYSIS OF CAPTURED THERMOGRAMS IN FRESH CONDITION AND THERE AFTER BRUISING THEM AFTER 7 AND 21 DAYS

| Statistical Feature Analysis of Thermograms Captured on the First Day   |                                  |          |                    |          |          |         |                                   |             |        |             |         |
|---|----------------------------------|----------|--------------------|----------|----------|---------|-----------------------------------|-------------|--------|-------------|---------|
| Sample No   | First Order Statistical Features |          |                    |          |          |         | Second Order Statistical Features |             |        |             |         |
|   | Mean                             | Variance | Standard Deviation | Skewness | Kurtosis | Entropy | Contrast                          | Correlation | Energy | Homogeneity | Entropy |
| 1   | 94.80                            | 4407.64  | 66.39              | 0.13     | 1.40     | 0.0027  | 0.1197                            | 0.1667      | 0.9305 | 0.9012      | 0.0027  |
| 2   | 92.73                            | 4235.91  | 65.08              | 0.05     | 1.35     | 0.0019  | 0.1224                            | 0.1641      | 0.9332 | 0.8971      | 0.9937  |
| 3   | 85.65                            | 4525.2   | 67.27              | 0.41     | 1.40     | 0.0044  | 0.1029                            | 0.2204      | 0.9360 | 0.9077      | 0.7856  |
| 4   | 81.15                            | 4246.1   | 65.16              | 0.44     | 1.39     | 0.0039  | 0.1304                            | 0.2312      | 0.9359 | 0.9050      | 0.6253  |
| 5   | 82.94                            | 4094.0   | 63.98              | 0.20     | 1.41     | 0.0035  | 0.1034                            | 0.2337      | 0.9452 | 0.9315      | 0.8960  |
| Statistical Feature Analysis of the Similar Thermograms after Bruising them in Normal Temperature after 7 Days  |                                  |          |                    |          |          |         |                                   |             |        |             |         |
| 1   | 106.12                           | 4861.1   | 69.72              | 0.14     | 1.49     | 0.0036  | 0.1710                            | 0.3408      | 0.9435 | 0.9094      | 0.8113  |
| 2   | 114.18                           | 6342.31  | 79.64              | 0.34     | 1.40     | 0.0077  | 0.1302                            | 0.2499      | 0.9381 | 0.9373      | 0.0077  |
| 3   | 117.72                           | 6525.73  | 80.78              | 0.43     | 1.42     | 0.0047  | 0.1306                            | 0.3009      | 0.9409 | 0.9284      | 0.0047  |
| 4   | 112.85                           | 6231.39  | 78.94              | 0.31     | 1.43     | 0.0042  | 0.1321                            | 0.2788      | 0.9384 | 0.9274      | 0.0042  |
| 5   | 111.42                           | 5915.47  | 76.91              | 0.35     | 1.44     | 0.0052  | 0.1130                            | 0.2585      | 0.9471 | 0.9319      | 0.0070  |
| Statistical Feature Analysis of the Similar Thermograms after Bruising them in Normal Temperature after 21 Days |                                  |          |                    |          |          |         |                                   |             |        |             |         |
| 1   | 123.44                           | 7127.06  | 84.42              | 0.49     | 1.58     | 0.0044  | 0.1886                            | 0.3409      | 0.9439 | 0.9553      | 0.9284  |
| 2   | 121.34                           | 6866.87  | 82.87              | 0.48     | 1.51     | 0.0099  | 0.1489                            | 0.3240      | 0.9433 | 0.9530      | 0.9130  |
| 3   | 120.93                           | 6918.83  | 83.18              | 0.51     | 1.57     | 0.0047  | 0.1548                            | 0.3259      | 0.9518 | 0.9437      | 0.9652  |
| 4   | 124.39                           | 7112.50  | 84.34              | 0.48     | 1.57     | 0.0056  | 0.1685                            | 0.3055      | 0.9394 | 0.9389      | 0.9422  |
| 5   | 122.09                           | 6936.61  | 83.29              | 0.41     | 1.53     | 0.0070  | 0.1219                            | 0.3156      | 0.9501 | 0.9452      | 0.9284  |

$$I_{(t+1)}(s) = I_t(s) + \frac{\lambda}{|n_s|} \sum_{p \in N_s} g_k \left( e^{-\left(\frac{|V_{I_t,p}|}{k}\right)^2} \right) (I_t(p) - I_t(s)) \quad (2)$$

Here,  $I$  is the discretely sampled image,  $s$  denotes the pixel position in the discrete 2D grid,  $t$  denotes the iteration step,  $g$  is the conduction function,  $k$  is the gradient threshold parameter,  $\lambda$  is constant and  $\lambda \in [0, 1]$ ,  $n_s$  denotes the no of spatial neighbours considered for the pixel  $s$ .

2) *Segmentation of the bruised region*: To calculate the spreadness of the bruised region, segmentation of that region from the whole thermograms is carried out using k-means clustering [14]. On the basis of analysis of the pre-processed thermograms it has been found that there are ten number of clusters depending on the color palette division of temperature distribution and maximum intensity is present in the bruised area. So the main aim of this algorithm is to minimize the objective function given by:

$$J = \sum_{j=1}^k \sum_{i=1}^n \|x_i^{(j)} - c_j\|^2 \quad (3)$$

Here  $\|x_i^{(j)} - c_j\|^2$  is a distance measure between a data point  $x_i^{(j)}$  and the cluster centre  $c_j$ .

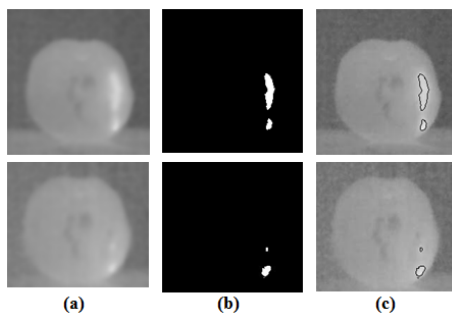


Fig. 6 Smoothing and Segmentation of the Bruised Area (a) Smoothened Image; (b) Segmented ROI; (c) Mapping of the Segmented ROI in the Original Image

## V. EXPERIMENTAL RESULTS AND DISCUSSIONS

### A. Statistical Feature analysis of thermograms

The statistical feature analysis was carried out on the first part of the database i.e. on 50 samples. After extracting these 11 feature values from both fresh (i.e. thermograms captured

on the first day) and bruised (i.e. thermograms captures after 7 and 21 days) apples, an analysis of the feature values are done to find out any asymmetric characteristics. The first order statistical feature values obtained from 5 randomly selected thermograms of both the category of apples are shown in TABLE II. From this analysis it has been found that in most of the cases the statistical feature values of the fresh apples is less than that of the apples bruised externally after 7 days and less than that of 21 days. Among all first order features mean, standard deviation and variance shows a better discrimination power but the significant difference of skewness, kurtosis and entropy is less. It has been found that the mean temperature value is less than 100 in case of all the fresh apples whereas the value is more than 100 in case of the bruised apples. After analyzing the first order feature values, the second-order features are also extracted and analyzed in both the category of thermograms as shown in TABLE II. Although, there is a asymmetric difference between the fresh and bruised thermograms, but these differences are not decisive. However among all these second order features it has been found the value of homogeneity and correlation shows better discrimination ability between the fresh and bruised thermograms of apples but there is no such asymmetric difference in the values of contrast. Thus, from the statistical feature based asymmetry analysis of the thermograms, it has been observed that intensity based histogram plays a crucial role in asymmetric analysis of the thermograms.

### B. Fractal features analysis of the thermograms

The fractal feature analysis of the thermograms has been done for asymmetric analysis between fresh and bruised apples. Because of the irregularity and heterogeneity present in the bruised apples they show higher values of fractal dimension. The analysis has been carried out on 10 fresh apples and 10 bruised apples and it has been observed that fractal feature values are higher in case of bruised apples than fresh apples as shown in TABLE III. In the given data it can be analyzed that the fractal dimension is higher, for example, less than 1.25 in case of fresh apples whereas more than 1.25 in case of bruised apples.

### C. Objective Validation of the Extracted Bruised Region:

After extraction of the bruised region from the whole thermogram, the objective evaluation of the segmented bruised regions is carried out based on the four metrics i.e.

TABLE III  
 FRACTAL ANALYSIS AND OBJECTIVE VALIDATION AND SPREADNESS MEASUREMENT OF EXTRACTED BRUISED REGION

| Sample No | Fractal Analysis of the Thermograms |               | Objective Validation of the Extracted Bruised Region |                                |                                |                                   | Spreadness Measurement |                   |
|-----------|-------------------------------------|---------------|--|--------------------------------|--------------------------------|-----------------------------------|------------------------|-------------------|
|           | Fresh Apple                         | Bruised Apple | Probability Rand Index (PRI)                         | Global Consistency Error (GCE) | Variation of Information (VOI) | Boundary Displacement Error (BDE) | Area                   | Fractal Dimension |
| 1         | 1.2252                              | 1.2760        | 0.9665   | 0.0020                         | 0.1200                         | 0.0130                            | 558                    | 0.8293            |
| 2         | 1.2076                              | 1.2679        | 0.9751   | 0                              | 0.1529                         | 0.0530                            | 155                    | 0.7386            |
| 3         | 1.2253                              | 1.2566        | 0.9776   | 0.0056                         | 0.1779                         | 0.0177                            | 2045                   | 0.9423            |
| 4         | 1.2045                              | 1.2715        | 0.9793   | 0.0053                         | 0.1113                         | 0.0790                            | 1798                   | 0.9154            |
| 5         | 1.1947                              | 1.2778        | 0.9879   | 0.0067                         | 0.1454                         | 0.0167                            | 2223                   | 0.9629            |
| 6         | 1.1917                              | 1.2941        | 0.9841   | 0.0045                         | 0.1404                         | 0.0444                            | 5178                   | 1.0507            |
| 7         | 1.2432                              | 1.2758        | 0.9786   | 0.0017                         | 0.1489                         | 0.0119                            | 1713                   | 0.9072            |
| 8         | 1.2474                              | 1.2935        | 0.9915   | 0.0019                         | 0.0705                         | 0.0782                            | 512                    | 0.8107            |
| 9         | 1.2367                              | 1.2796        | 0.9863   | 0.0034                         | 0.1227                         | 0.0835                            | 1043                   | 0.8653            |
| 10        | 1.1230                              | 1.2989        | 0.9553   | 0.0037                         | 0.1353                         | 0.0567                            | 1763                   | 0.9083            |

Probability Rand Index (PRI), Variation of Information (VoI), Global Consistency Error (GCE) and Boundary Displacement Error (BDE) [15]. Among this four performance metric, in case of PRI higher probability is better whereas in case of the remaining three metric the lower distance is better.

Each of this performance metrics are measured by comparing the automated detected bruised region with the manually segmented bruised region i.e. the ground truth images that are created by the human observer. Digitized manually drawn segmented region is obtained using the software GIMP (GNU Image Manipulation Program) [16]. The proposed results (i.e. automated extracted region) are compared with these reference ground truth and this comparison is given in TABLE III. From the objective evaluation it is clear that PRI is about 0.8827 on average which is almost close to 1 and other three metrics i.e. VoI, GCE and BDE on average are 0.0003, 0.1192 and 0.0397 respectively which seems to be more highly or nearly correlated with human hand segmentations i.e. the ground truth images.

#### D. Spreadness Measurement of the Extracted Bruised Region:

After validation of the detected ROI, the spreadness measurement of the extracted bruised region is carried out in terms of area and fractal dimension. Areas are calculated as the total number of pixels in the extracted region and fractal dimensions are calculated using the box counting method. The spreadness measurement of the extracted bruised region is shown in TABLE III. Here spreadness measurement of image no 1 and 2 are the corresponding outputs of the extracted bruised region shown in Fig. 5. So we can see that since area of the bruised region in image 1 is more as compared to image 2 so its corresponding fractal dimension is also more and with the increase of the bruised region its corresponding fractal dimension also increases as shown in TABLE III.

## VI. CONCLUSION

Here we have presented a methodology for asymmetric analysis of the thermograms (i.e. bruised and fresh apples) and automatic segmentation of the bruised region and measure its spreadness. The temperature based statistical and fractal analysis shows that the feature values of the fresh apples is less than that of the bruised apples bruised. Also after automatic segmentation of the bruised region, validation of the extracted region is measured using four metric and spreadness of the extracted bruised region is measured in terms of fractal dimension.

## ACKNOWLEDGMENT

The work presented here is being conducted in the Bio-Medical Infrared Image Processing Laboratory (B-MIRD), of

Computer Science and Engineering Department, Tripura University (A Central University), Suryamaninagar-799022, Tripura (W). The research work is supported by the Grant No. BT/533/NE/TBP/2013, Dated 03/03/2014 from the Department of Biotechnology (DBT), Government of India.

## REFERENCES

- [1] FDA approves GMO apples, potatoes that don't bruise or brown as being safe to eat. [Online]. Available: <https://www.rt.com/usa/243065-fda-approves-gmo-apples/>.
- [2] L. Qiang, and T. Mingjie, "Detection of hidden bruise on kiwi fruit using hyperspectral imaging and parallelepiped classification," in *Procedia Environmental Sciences*, 2012, Vol. 12, pp. 1172-1179.
- [3] J. Varith, G.M. Hyde, A.L. Baritelle, J.K. Fellman and T. Sattabongkot, "Non-contact bruise detection in apples by thermal imaging," *Innovative Food Science & Emerging Technologies*, Vol. 4, No. 2, pp. 211-218, June 2013.
- [4] P. Baranowski, W. Mazurek, B.W. Walczak and C. Slawinski, "Detection of early apple bruises using pulsed-phase thermography," *Postharvest biology and technology*, Vol. 53, No. 3, pp. 91-100, Sept. 2009.
- [5] J. Xing, C. Bravo, P.T. Jancsok, H. Ramon, B. J.D. Baerdemaeker, "Detecting Bruises on 'Golden Delicious' Apples using Hyperspectral Imaging with Multiple Wavebands," *Biosystems Engineering*, Vol. 90, No. 1, pp. 27-36, Jan. 2005.
- [6] B.L. Upchurch, J. A. Throop, and D. J. Aneshansley, "Influence of time, bruise-type, and severity on near-infrared reflectance from apple surfaces for automatic bruise detection," *Transactions of the ASAE*, Vol. 37, No. 5, pp. 1571-1575, 1994.
- [7] B.S. Bennedson and D. L. Peterson, "Performance of a system for apple surface defect identification in near-infrared image," *Biosystems Engineering*, Vol. 90, No. 4, pp. 419-431, April 2005.
- [8] J. Xing, P. Jancsó, and Josse De Baerdemaeker, "Stem-end/calyx identification on apples using contour analysis in multispectral images," *Biosystems Engineering*, Vol. 96, No. 2, pp. 231-237, Feb. 2007.
- [9] G. ElMasry, N. Wang, C. Vigneault, J. Qiao and A. ElSayed, "Early detection of apple bruises on different background colors using hyperspectral imaging," *LWT-Food Science and Technology*, Vol. 41, No. 2, pp. 337-345, March 2008.
- [10] P. Baranowski, W. Mazurek, J. Wozniak and U. Majewska, "Detection of early bruises in apples using hyperspectral data and thermal imaging," *Journal of Food Engineering*, Vol. 110, No. 3, pp. 345-355, June 2012.
- [11] N. Aggarwal and R. K. Agrawal, "First and second order statistics features for classification of magnetic resonance brain images," *Journal of Signal and Information Processing*, Vol. 3, No. 2, pp. 146-153, 2012.
- [12] F. Kenneth, "Fractal geometry: mathematical foundations and applications," John Wiley & Sons, 2004.
- [13] P. Perona and J. Malik, "Scale-space and edge detection using anisotropic diffusion," *IEEE Transactions on Pattern Analysis and Machine Intelligence*, Vol. 12, No. 7, pp. 629-639, July 1990.
- [14] N. Shi, L. Xumin, and G. Yong, "Research on k-means clustering algorithm: An improved k-means clustering algorithm," 2010 Third International Symposium on Intelligent Information Technology and Security Informatics (IITSI), IEEE, pp. 63-67, 2010.
- [15] M. Mignotte, Max, "Segmentation by fusion of histogram-based-means clusters in different color spaces," *IEEE Transactions on Image Processing*, Vol. 17, No. 5, pp. 780-787, May 2008.
- [16] R.W. Solomon, "Free and open source software for the manipulation of digital images," *American Journal of Roentgenology*, Vol. 192, No. 6, pp. W330-W334, June 2009.